Supporting Information

Universal Relationship between Conductivity and Solvation-Site Connectivity Ether-based Polymer Electrolytes

Danielle M. Pesko,[†1] Michael A. Webb,[‡1] Yukyung Jung,[∥1] Qi Zheng,[∥] Thomas F. Miller III,[‡*] Geoffrey W. Coates,[∥*] and Nitash P. Balsara[†,§,⊥*]

[†] *Department of Chemical and Biomolecular Engineering, University of California, Berkeley, California 94720, USA*

[‡] *Division of Chemistry and Chemical Engineering, California Institute of Technology, Pasadena, California 91125, USA*

[∥] *Department of Chemistry and Chemical Biology, Baker Laboratory, Cornell University, Ithaca, New York 14853, USA*

[§] *Materials Science Division, Lawrence Berkeley National Laboratory, Berkeley, California 94720, USA*

[⊥] *Environmental Energy Technology Division, Lawrence Berkeley National Laboratory, Berkeley, California 94720, USA*

[1]These authors contributed equally to the work.

Contents

1 Synthesis Details

1.1 General Considerations

All manipulation of air and water sensitive compounds were carried out under dry nitrogen using a Braun Labmaster Glovebox or standard Schlenk line techniques. ^{1}H and ^{13}C NMR spectra were recorded on Varian INOVA 400 (^{1}H, 400 MHz) or Varian INOVA 500 (^{1}H, 500 MHz) spectrometers. ^{1}H NMR spectra were referenced with residual non-deuterated solvent shifts ($CHCl_3$=7.26 ppm), and ^{13}C NMR spectra were referenced by the deuterated solvent shifts ($CDCl_3$=77.16 ppm).

Flash column chromatography was performed using silica gel with particle size 40-64 μm, 230-400 mesh. Gel permeation chromatography (GPC) analyses were done using an Agilent PL-GPC 50 integrated system (2 x Plgel Mini-MIX C columns, 5 micron, 4.6 mmID) equipped with a refractive index detector. The GPC columns were eluted with tetrahydrofuran at a rate of 0.3 mL/min at 30 ºC, and calibration was done using monodisperse polystyrene standards.

Differential Scanning Calorimetry (DSC) of polymer samples was performed on a TA Instruments Q1000 modulated differential scanning calorimeter with a 50 chamber autosampling platform. Samples were prepared in crimped aluminum pans, and experiments were conducted using the following protocol unless otherwise stated: heating under nitrogen from 25 ºC to 200 ºC at 10 ºC/min, cooling from 200 to -100 ºC at 10 ºC/min, and then heating from -100 to 200 ºC at 10 ºC/min. The data were processed using Universal Analysis 2000 software, and all reported glass transition temperatures (T_g) and melting temperatures (T_m) were obtained from the second heating cycle. Thermal gravimetric analysis (TGA) was performed using a TA Instruments Q500 Thermogravimetric Analyzer equipped with an autosampler. HRMS Analyses were performed on a Thermo Scientific Exactive Orbitrap MS system with an Ion Sense DART ion source.

1.2 Materials

Grubbs first generation catalyst (Sigma-Aldrich or Strem) and Crabtree's catalyst (Sigma-

Aldrich) were stored under nitrogen in the glovebox and used as received. Diethylene glycol (Sigma-Aldrich, 99%) was dried over activated 3 Å molecular sieves overnight then vacuum distilled. Triethylene glycol (Sigma-Aldrich, 99%) and tetraethylene glycol (Sigma-Aldrich, 99%) were dried over activated 3 Å molecular sieves overnight. Tetrahydrofuran (THF) and dichloromethane (DCM) were obtained from Fisher Scientific and dimethylformamide (DMF) was obtained from Burdick and Jackson, and the solvents were dried using a Phoenix solvent drying system. Alumina beads (F-200, BASF) were activated by heating to 180 °C overnight under reduced pressure, then stored in the glovebox. All other reagents were purchased from commercial sources and used as received.

1.3 Synthesis of Monomers

1.3.1 Synthesis of $C_2EO_4\pi$ Monomer

In the glovebox, sodium hydride (95%, 2.7 g, 112 mmol) was added to a 500 mL vacuum-adapted round bottom flask with a stirbar. The flask was sealed and taken out of the glovebox, and THF (200 mL) was added via cannula under nitrogen. Triethylene glycol (6.0 mL, 44 mmol) was added dropwise and stirred for 20 minutes at room temperature. Allyl bromide (8.0 mL, 92.4 mmol) was added dropwise, and the reaction was stirred overnight. The reaction was concentrated in vacuo, and the residue was suspended in 150 mL of ether. The ether layer was washed three times with water, dried over magnesium sulfate, and concentrated. The crude product was purified by column chromatography using 50% ether in hexanes as the eluent. The product was obtained in 57% yield (5.76 g, 25.0 mmol), and stored neat over activated alumina beads in the glovebox. The ^{1}H NMR spectrum of the product matched well with literature values.[1] ^{1}H NMR spectrum in ppm ($CDCl_3$, 500 MHz): δ 5.97-5.84 (ddt, *J*=5.7 Hz, 5.7 Hz, 10.5Hz, 21.9 Hz, 2H); 5.26 (dd, J=1.6 Hz, 17.2 Hz, 2H); 5.17 (dd, J=1.24 Hz, 10.4 Hz, 2H); 4.01 (d, J=2.7 Hz, 4H); 3.71-3.50 (m, 12 H). ^{13}C NMR spectrum in ppm ($CDCl_3$, 125 MHz): δ 134.88, 117.22, 72.36, 70.76, 69.54. HR/MS (DART): calculated for $C_{12}H_{23}O_4^+$ $(M+H)^+$ 231.1591 g/mol; found 231. 1590 g/mol.

1.3.2 Synthesis of $C_2EO_5\pi$ Monomer

Tetraethylene glycol diallyl ether was synthesized following a procedure adapted from the literature.[2] In the glovebox, sodium hydride (1.24 g, 51.5 mmol) was added to a 100 mL round bottom flask with a stirbar. The flask was removed from the glovebox, and 20 mL of dry degassed DMF was added via syringe. The flask was cooled to 0 ˚C, and tetraethylene glycol was added dropwise (2.0 g, 10.3 mmol). The reaction was stirred at 0 ˚C for 15 minutes, then allyl glycidyl ether (3.48 mL, 40.2 mmol) was added dropwise. The flask was warmed to room temperature and stirred overnight. The reaction was quenched with isopropanol, filtered through a Celite plug, and diluted with ~100 mL ether. The solution was washed three times with brine, dried over sodium sulfate, and concentrated. The crude product was purified by column chromatography with 100% diethyl ether as the eluent. The product was obtained in 77% yield (2.18 g, 7.9 mmol), and stored neat over activated alumina beads in the glovebox. ^{1}H NMR spectrum in ppm ($CDCl_3$, 500 MHz): δ 5.90 (ddd, J=5.7 Hz, 10.9 Hz, 22.8 Hz, 2H); 5.26 (dd, J=1.3 Hz, 17.2 Hz, 2H); 5.17 (d, J=10.4 Hz, 2H); 4.01 (d, J=5.7 Hz, 4H); 3.75-3.52 (m, 1H). ^{13}C NMR spectrum in ppm ($CDCl_3$, 125 MHz): δ 134.88, 117.22, 72.36, 70.76, 70.72, 69.54. HR/MS (DART): calculated for $C_{14}H_{27}O_5^+$ $(M+H)^+$ 275.1853 g/mol; found 275.1850 g/mol.

1.3.3 Synthesis of $C_4EO_4\pi$ Monomer

The synthesis of the mesyl-terminated PEG was adapted from a literature procedure.[3] Triethylene glycol (3 g, 20 mmol) was added to a 300 mL vacuum adapted round bottom flask equipped with a stirbar under nitrogen. Dry dichloromethane (100 mL) and diisopropylethylamine (7.7 mL, 44 mmol) were added via cannula, and the flask was cooled to 0 ˚C. The solution was stirred for 10 minutes, and then methanesulfonyl chloride (3.4 mL, 44 mmol) was added. The flask was allowed to warm to room temperature and stirred overnight. The crude reaction mixture was washed with 100 mL brine, and the organic layer was concentrated under reduced pressure. The residue was partitioned between 100 mL hexanes and 100 mL water. Sodium chloride (10 g) was added to the aqueous layer,

which was extracted with 3x100 mL dichloromethane. The combined organic layers were dried over sodium sulfate and concentrated. The crude product was purified by column chromatography using 5% methanol in dichloromethane as the eluent. The product was isolated as a yellow oil in 29% yield (1.77 g, 5.8 mmol), and the ^{1}H NMR spectrum was consistent with the literature. ^{1}H NMR spectrum in ppm ($CDCl_3$, 400 MHz): δ4.37 (m, 4H), 3.76 (m, 4H), 3.67 (s, 4H), 3.07 (s, 6H).

In the glovebox, sodium hydride (95%, 253 mg, 10.5 mmol) was added to a 20 mL scintillation vial equipped with a stirbar. The vial was sealed with a pierceable Teflon-lined septum cap and brought out of the glovebox. Dry THF (5 mL) was added via syringe .The reaction was cooled to 0 ˚C, then 3-butene-1-ol (800 μL, 9.3 mmol) was added dropwise and stirred for 15 minutes. The mesyl-terminated PEG (1.48 g, 4.8 mmol) was dissolved in 5 mL THF, and the solution was added to the vial dropwise. The reaction was warmed to room temperature and stirred overnight. The vial was quenched with H_2O and concentrated under reduced pressure. Diethyl ether (80 mL) was added to the residue, and the milky suspension was filtered through Celite and concentrated. The crude product was purified by column chromatography using 50% ether in hexanes as the eluent. The product was isolated as a clear oil in 36% yield (0.90 g, 1.7 mmol), and stored over activated alumina beads in the glovebox. ^{1}H NMR spectrum in ppm ($CDCl_3$, 500 MHz): δ 5.82 (ddt, J=6.8 Hz, 6.8 Hz, 10.2 Hz, 17.0 Hz, 2H); 5.09 (dd, J=1.5 Hz, 17.2 Hz, 2 H); 5.04 (d, J=10.2 Hz, 2H); 3.70-3.58 (m, 12 H); 3.53 (t, J=6.9 Hz, 4H); 2.35 (q, J=6.8 Hz, 4H). ^{13}C NMR spectrum in ppm ($CDCl_3$, 125 MHz): δ 135.27, 116.44, 70.77, 70.75, 70.70, 70.26, 34.25. HR/MS (DART): calculated for $C_{14}H_{27}O_4^+$ $(M+H)^+$ 259.1909 g/mol; found 259.1903 g/mol.

1.3.4 Synthesis of $C_4EO_5\pi$ Monomer

The $C_4EO_5\pi$ monomer was synthesized using the same procedure as for $C_4EO_4\pi$, except tetraethylene glycol was used instead of triethylene glycol. The monomer was purified by column chromatography using 50 to 75% ether in hexanes as the eluent. The product was isolated as a clear oil

in 46% yield (0.66 g, 1.44 mmol), and stored over activated alumina beads in the glovebox. ^{1}H NMR spectrum in ppm ($CDCl_3$, 500 MHz): δ 5.81(ddt, J=6.7 Hz, 6.7 Hz, 10.2 Hz, 17.0 Hz, 2H); 5.08 (dd, J=1.8 Hz, 17.2 Hz, 2H); 5.02 (d, J=10.2 Hz, 2H); 3.68-3.56 (m, 18 H); 3.51 (t, J=6.9 Hz, 4H), 2.34 (qd, J=5.6 Hz, 6.8 Hz, 6.9 Hz, 6.9 Hz, 4H). ^{13}C NMR spectrum in ppm ($CDCl_3$, 125 MHz): δ 135.27, 116.46, 70.78, 70.74, 70.72, 70.70, 70.26, 34.25. HR/MS (DART): calculated for $C_{16}H_{31}O_5^+$ $(M+H)^+$ 303.2166 g/mol; found 303.2165 g/mol.

1.3.5 Synthesis of $C_6EO_4\pi$ Monomer

The synthesis of the $C_6EO_4\pi$ monomer was adapted from a literature procedure.[4] In the glovebox, sodium hydride (95%, 288 mg, 12 mmol) was added to a 20 mL scintillation vial equipped with a stirbar. The vial was sealed with a pierceable Teflon-lined septum cap and brought out of the glovebox. Under nitrogen, sodium iodide (37 mg, 0.24 mmol) and dry THF (5 ml) were added (mg, mmol), and the vial was cooled to 0 ˚C. Triethylene glycol (0.54 mL, 4.0 mmol) was added dropwise, and the reaction was stirred until the bubbling ceased (~5 minutes). The 5-bromo-1-pentene (1.42 mL, 12 mmol) was added dropwise as a solution in 6 mL THF. The reaction was allowed to warm to room temperature and stirred 5 days. The crude reaction mixture was concentrated under reduced pressure. The residue was diluted in 10 mL diethyl ether, filtered through Celite, and concentrated. The crude product was purified by column chromatography using 33 to 50% diethyl ether in hexanes as the eluent. The product was obtained as a clear oil in 31% yield (354 mg, 1.24 mmol) and stored over activated alumina beads in the glovebox. ^{1}H NMR spectrum in ppm ($CDCl_3$, 500 MHz): δ 5.82 (ddt, J=6.6 Hz, 6.6 Hz, 10.2 Hz, 16.9 Hz, 2H); 5.03 (dd, J=1.64 Hz, 17.1 Hz, 2H); 4.97 (d, J=10.2 Hz, 2H); 3.70-3.57 (m, 8H); 3.48 (t, J=6.7 Hz, 4H); 2.12 (dd, J=7.3 Hz, 14.3 Hz, 4H); 1.69 (m, 4H). ^{13}C NMR spectrum in ppm ($CDCl_3$, 125 MHz): δ 138.43, 114.81, 70.84, 70.76, 70.24, 30.37, 28.91. HR/MS (DART): calculated for $C_{16}H_{31}O_4^+$ $(M+H)^+$ 287.2217 g/mol; found 287.2215 g/mol.

1.3.6 Synthesis of $C_6EO_5\pi$ Monomer

The $C_6EO_5\pi$ monomer was synthesized using the same procedure as for $C_6EO_4\pi$, except tetraethylene glycol was used instead of triethylene glycol. The crude product was purified by column chromatography using 50 to 75% ether in hexanes as the eluent. The product was isolated as a clear oil in 35% yield (459 mg, 1.4 mmol), and stored over activated alumina beads in the glovebox. ^{1}H NMR spectrum in ppm ($CDCl_3$, 500 MHz): δ 5.80 (ddt, J=6.6 Hz, 6.6 Hz, 10.2 Hz, 13.3 Hz, 2 H); 5.00 (d, J=17.1 Hz, 2H); 4.94 (d, J=10.1 Hz, 2H); 3.78-3.52 (m, 12H); 3.45 (t, J=6.7 Hz, 4H); 2.10 (dd, J=7.0 Hz, 14.3 Hz, 4H); 1.67 (m, 4H). ^{13}C NMR spectrum in ppm ($CDCl_3$, 125 MHz): δ 138.41, 114.81, 70.83, 7074, 70.23, 30.36, 28.90. HR/MS (DART): calculated for $C_{18}H_{35}O_5^+$ $(M+H)^+$ 331.2479 g/mol; found 331.2477 g/mol.

1.4 Synthesis of Polymers

1.4.1 Representative ADMET Procedure for Unsaturated Polyethers

In the glovebox, Grubbs first generation catalyst (11.2 mg, 13.6 μmol) was added to a 100 mL vacuum-adapted round bottom flask equipped with a 1' stirbar. Neat triethylene glycol diallyl ether ($C_2EO_4\pi$, 200 mg, 0.87 mmol) was added via Pasteur pipet. Dry, degassed dichloromethane (~0.5 mL) was used to rinse the sides of the flask and pipet. The flask was sealed and brought outside of the glovebox. On the Schlenk line, the dichloromethane was removed under reduced pressure at room temperature while stirring. After ~1 minute, the reaction was left open to vacuum and heated to 50 ˚C for 2 hours. The polymerization was quenched by cooling the reaction to room temperature under nitrogen, then rapidly adding 0.5 mL ethyl vinyl ether via syringe. The reaction was then stirred at room temperature for at least 30 minutes before precipitating into 15 mL of stirring hexanes. The hexanes were decanted from the precipitated polymer, which was dried at room temperature under reduced pressure. The polymer was isolated as a brown tacky goo in 87% yield.

1.4.2 Synthesis of Unsaturated $[C_2EO_5\pi]_n$ Polymer

The unsaturated $[C_2EO_5\pi]_n$ polymer was synthesized by following the representative ADMET procedure with the $C_2EO_5\pi$ monomer (400 mg, 1.5 mmol) and Grubbs first generation catalyst (19.2 mg, 23.3 μmol). The polymerization was run for 2 hours at 50 ˚C under reduced pressure, and the polymer was precipitated in hexanes and isolated as a brown goo in 64% yield (231.0 mg).

1.4.3 Synthesis of Unsaturated $[C_4EO_4\pi]_n$ Polymer

In the glovebox, Grubbs first generation catalyst (10.2 mg, 12.4 μmol) was added to a 100 mL vacuum-adapted round bottom flask equipped with a 1' stirbar. Neat $C_4EO_4\pi$ monomer (200 mg, 0.77 mmol) was added via Pasteur pipet. Dry, degassed dichloromethane (~0.5 mL) was used to rinse the sides of the flask and pipet. The flask was sealed and brought outside of the glovebox. On the Schlenk line, the dichloromethane was removed under reduced pressure at room temperature while stirring. After ~1 minute, the reaction was left open to vacuum and heated to 50 ˚C for 2 hours. After 2 hours, a solution of Grubbs first generation catalyst (1.3 mg, 1.6 μmol) in 0.5 mL dry, degassed dichloromethane was added via syringe under nitrogen, and the polymerization was continued for 2 hours at 50 ˚C under vacuum. The polymerization was quenched by cooling the reaction to room temperature under nitrogen, then rapidly adding 0.5 mL ethyl vinyl ether via syringe. The reaction was then stirred at room temperature for at least 30 minutes before precipitating into 15 mL of stirring hexanes. The hexanes were decanted from the precipitated polymer, which was dried at room temperature under reduced pressure. The polymer was isolated as a brown goo in 71% yield (125.8 mg).

1.4.4 Synthesis of Unsaturated $[C_4EO_5\pi]_n$ Polymer

The unsaturated $[C_4EO_5\pi]_n$ polymer was synthesized following the same procedure as for the unsaturated $[C_4EO_4\pi]_n$ polymer, except using the $C_4EO_5\pi$ monomer (200 mg, 0.66 mmol) and Grubbs first generation catalyst (8.7 mg, 10.6 μmol), followed by a second addition of Grubbs catalyst in 0.5

mL dichloromethane after 2 hours (1.3 mg, 1.6 μmol). The reaction was quenched with ethyl vinyl ether 2 hours after the second addition of catalyst and stirred for at least 30 minutes. The polymer was isolated as a brown goo in 81% yield (147.4 mg).

1.4.5 Synthesis of Unsaturated $[C_6EO_4\pi]_n$ Polymer

In the glovebox, Grubbs first generation catalyst (10.3 mg, 12.5 μmol) was added to a 100 mL vacuum-adapted round bottom flask equipped with a 1' stirbar. Neat $C_6EO_4\pi$ monomer (220 mg, 0.77 mmol) was added via Pasteur pipet. Dry, degassed dichloromethane (~0.5 mL) was used to rinse the sides of the flask and pipet. The flask was sealed and brought outside of the glovebox. On the Schlenk line, the dichloromethane was removed under reduced pressure at room temperature while stirring. After ~1 minute, the reaction was left open to vacuum and heated to 50 ˚C for 1 hour. The polymerization was quenched by cooling the reaction to room temperature under nitrogen, then rapidly adding 0.5 mL ethyl vinyl ether via syringe. The reaction was then stirred at room temperature for at least 30 minutes before precipitating into 15 mL of stirring hexanes. The hexanes were decanted from the precipitated polymer, which was dried at room temperature under reduced pressure. The polymer was isolated as a brown tacky goo in 56% yield (109.0 mg).

1.4.6 Synthesis of Unsaturated $[C_6EO_5\pi]_n$ Polymer

The unsaturated $[C_6EO_5\pi]_n$ polymer was synthesized following the same procedure as for the unsaturated $[C_6EO_4\pi]_n$ except using the $C_6EO_5\pi$ monomer (220 mg, 0.66 mmol) with Grubbs first generation catalyst (9.0 mg, 10.9 μmol). The polymerization was run for 1 hour, quenched with ethyl vinyl ether, and precipitated in hexanes. The polymer was isolated as a brown tacky goo in 78% yield (156.7 mg).

1.4.7 Representative Hydrogenation Procedure

In the glovebox, unsaturated $[C_2EO_4\pi]_n$ polymer (from $C_2EO_4\pi$ monomer, 600 mg unsaturated

polymer, 3.0 mmol repeat units) and Crabtree's catalyst (52 mg, 65 μmol) were dissolved in 100 mL dry dichloromethane. The solution was added to a Fischer-Porter bottle with a stirbar, and the reactor head was attached. The Fischer-Porter bottle was removed from the glovebox and charged with 30 psig of hydrogen. The reaction was stirred at room temperature for 20 hours, and then the reactor was vented to atmospheric pressure. The solvent was removed under reduced pressure to yield the hydrogenated polymer as a brownish grey tacky goo in quantitative yield.

1.4.8 Procedure for Removal of Ruthenium Residues from Polymer

The procedure for removing residual Ru was adapted from a literature procedure.[5] The polymer was dissolved in dichloromethane to give a concentration of ~50 mg/mL. Activated carbon (Darco KB 100 mesh wet powder, Sigma-Aldrich) was added (100 mass % relative to polymer), and the suspension was stirred at room temperature overnight. The slurry was filtered through a plug of Whatman glass microfiber filter paper cotton wool, and then concentrated under reduced pressure.

1.5 NMR Spectra of Polymers

1.5.1 NMR Spectra of Unsaturated $[C_2EO_4\pi]_n$

^{1}H NMR spectrum in ppm ($CDCl_3$, 400 MHz): δ 6.27 (dd, *J*=29.8, 12.6 Hz, endgroup); 5.85-5.75 (m, *trans* alkene, 2H including *cis* alkene); 5.73-5.67 (m, *cis*-alkene); 4.80-4.67 (m, endgroup); 4.10-3.95 (m, 4H); 3.71-3.51 (m, 13 H); 2.18 (q, *J*=7.2, 7.2, 7.2 Hz, endgroup); 1.53 (dd, *J*=6.7, 1.5 Hz, endgroup). ^{13}C NMR spectrum in ppm ($CDCl_3$, 125 MHz): δ 129.66, 129.49, 71.32, 70.72, 69.66, 69.59, 66.99, 28.37 (endgroup).

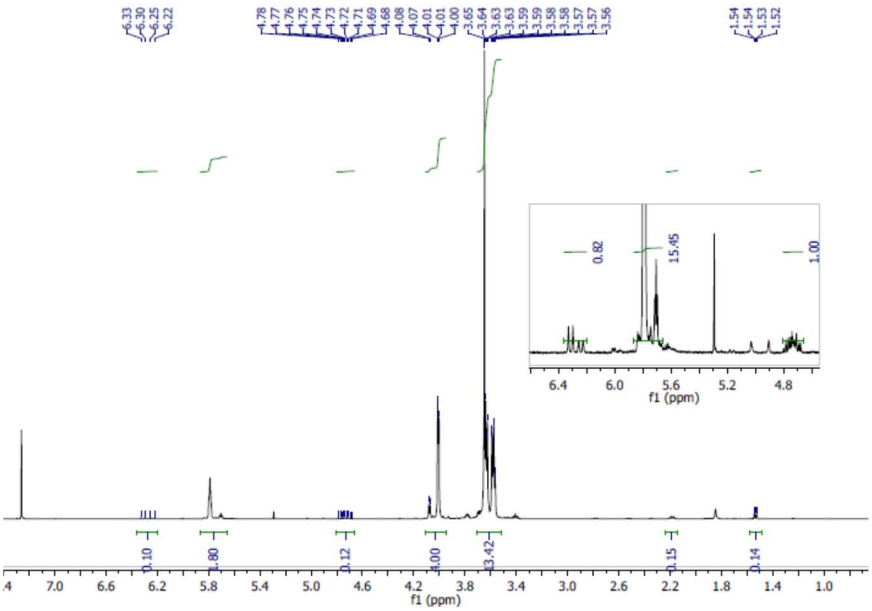

Figure 1. ^{1}H NMR spectrum of unsaturated $[C_2EO_4\pi]_n$ polymer in $CDCl_3$.

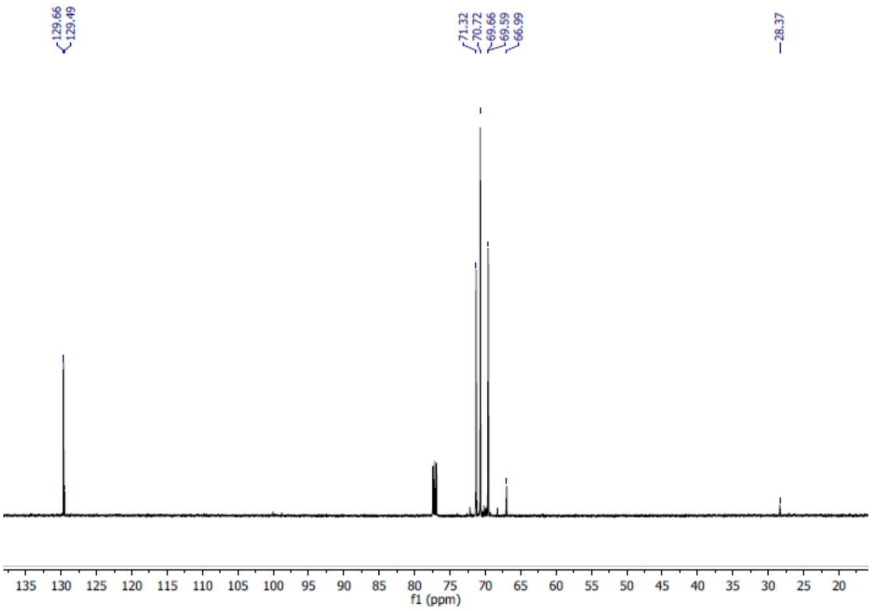

Figure 2. ^{13}C NMR spectrum of unsaturated $[C_2EO_4\pi]_n$ polymer in $CDCl_3$.

1.5.2 NMR Spectra of $[C_2EO_4]_n$

^{1}H NMR spectrum in ppm ($CDCl_3$, 500 MHz): δ 3.70-3.51 (m, 12 H); 3.50-3.40 (m, 4H); 1.69-1.56 (m, 4H); 0.90 (t, *J*=7.4, 7.4 Hz, endgroup). ^{13}C NMR spectrum in ppm ($CDCl_3$, 125 MHz): δ 71.26, 70.73, 70.19 26.39.

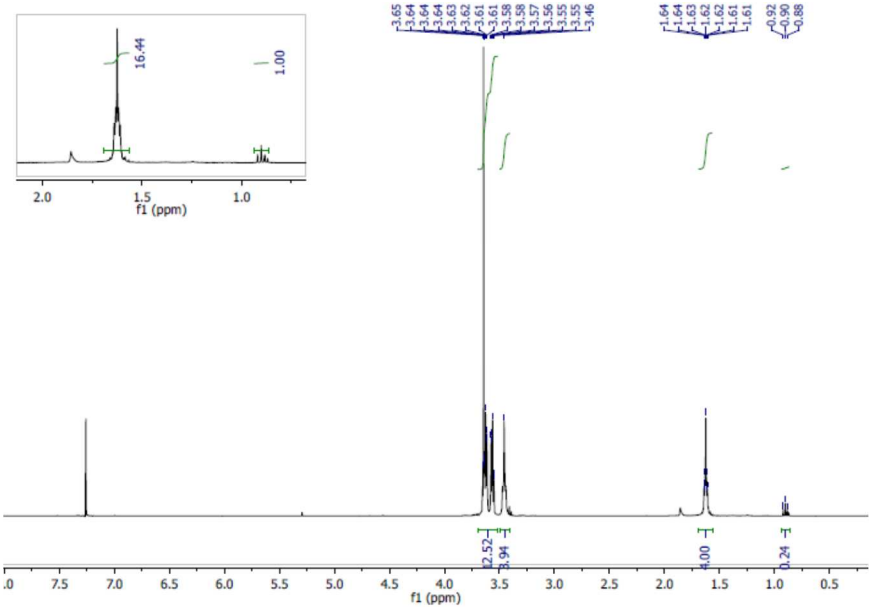

Figure 3. ^{1}H NMR spectrum of $[C_2EO_4]_n$ polymer in $CDCl_3$.

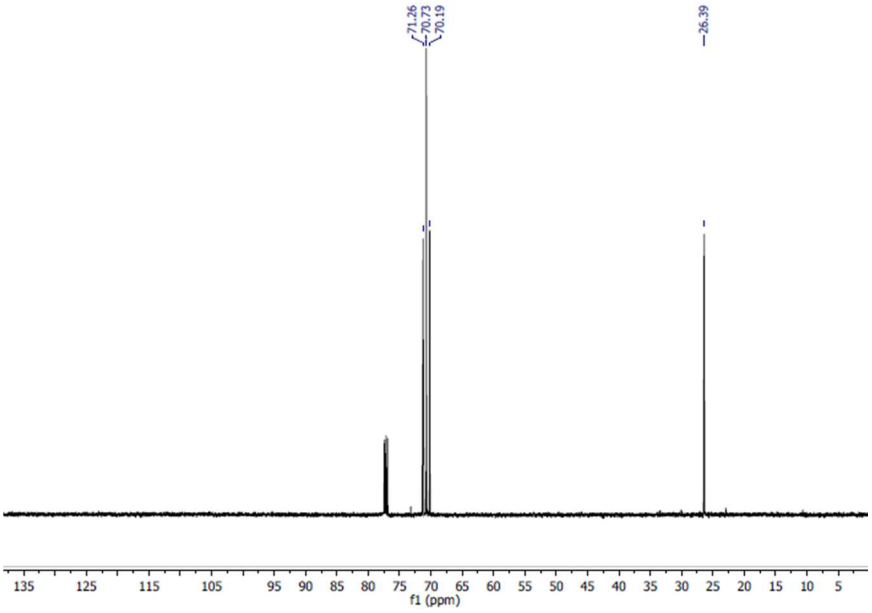

Figure 4. ^{13}C NMR spectrum of $[C_2EO_4]_n$ polymer in $CDCl_3$.

1.5.3 NMR Spectra of Unsaturated $[C_2EO_5\pi]_n$

^{1}H NMR spectrum in ppm ($CDCl_3$, 500 MHz): δ 5.89 (ddt, *J*=17.2, 10.4, 5.7 Hz, endgroup); 5.79-5.75 (m, *trans* alkene, 2H including *cis* alkene); 5.70-5.67 (m, *cis*-alkene); 5.27-5.12 (m, endgroup); 4.10-3.93 (m, 4H); 3.73-3.47 (m, 18H); 1.52 (dd, *J* = 6.7, 1.6 Hz, endgroup). ^{13}C NMR spectrum in ppm ($CDCl_3$, 125 MHz): δ 129.59, 71.26, 70.71, 70.70, 70.67, 69.65, 69.59, 66.97.

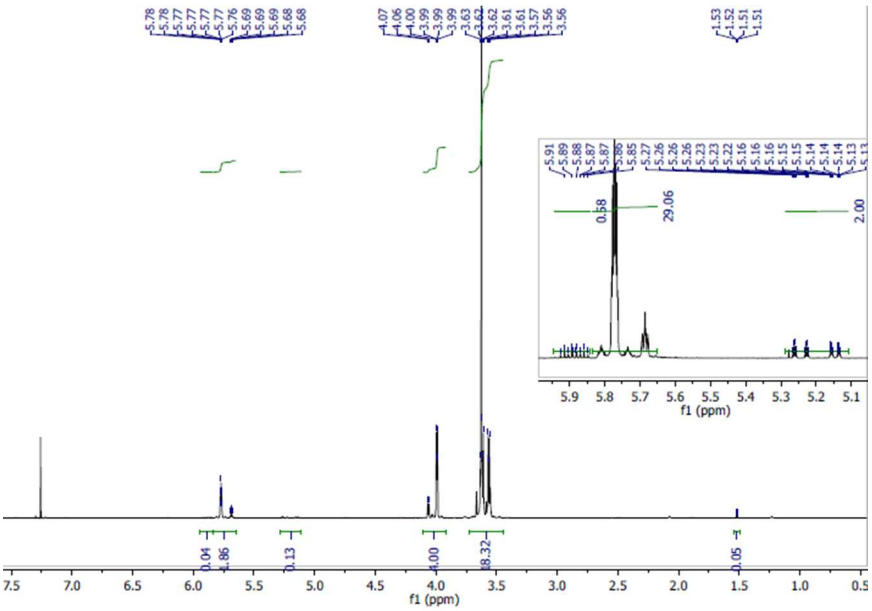

Figure 5. ^{1}H NMR spectrum of unsaturated $[C_2EO_5\pi]_n$ polymer in $CDCl_3$.

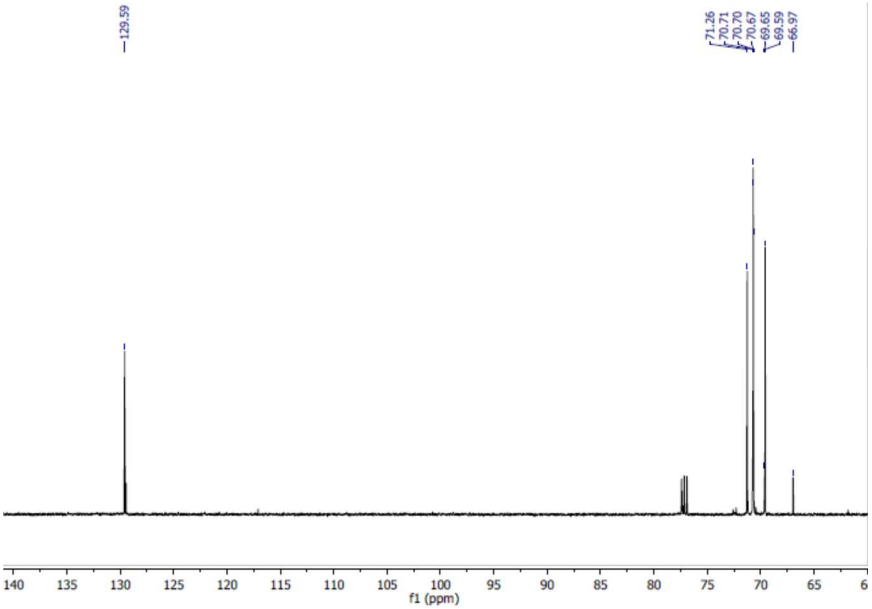

Figure 6. ^{13}C NMR spectrum of unsaturated $[C_2EO_5\pi]_n$ in $CDCl_3$.

1.5.4 NMR Spectra of $[C_2EO_5]_n$

^{1}H NMR spectrum in ppm ($CDCl_3$, 500 MHz): δ 3.70-3.53 (m, 19H); 3.50-3.42 (m, 4H); 1.68-1.56 (m, 4H); 0.89 (t, *J*=7.4, 7.4 Hz, endgroup). ^{13}C NMR spectrum in ppm ($CDCl_3$, 125 MHz): δ 71.28, 70.78, 70.24, 26.44**.**

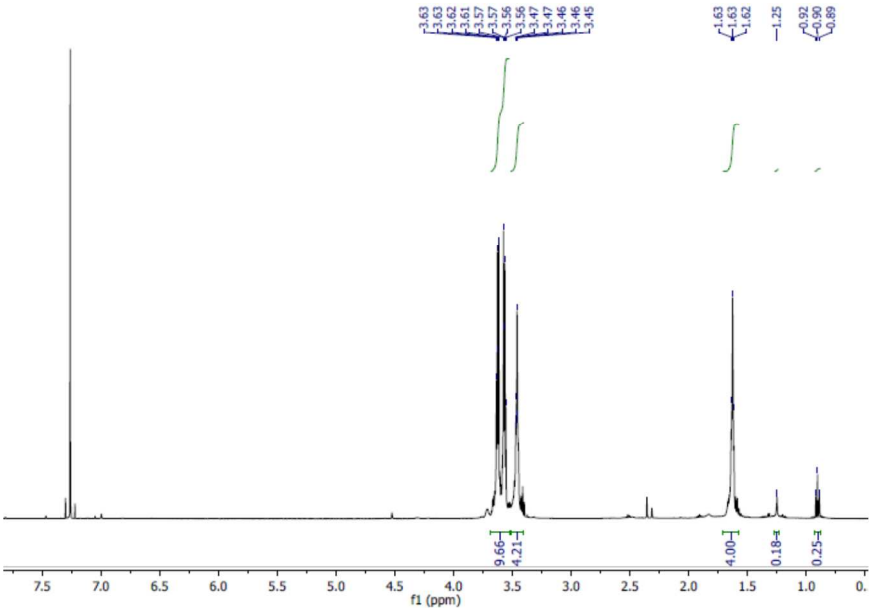

Figure 7. ^{1}H NMR spectrum of $[C_2EO_5]_n$ polymer in $CDCl_3$.

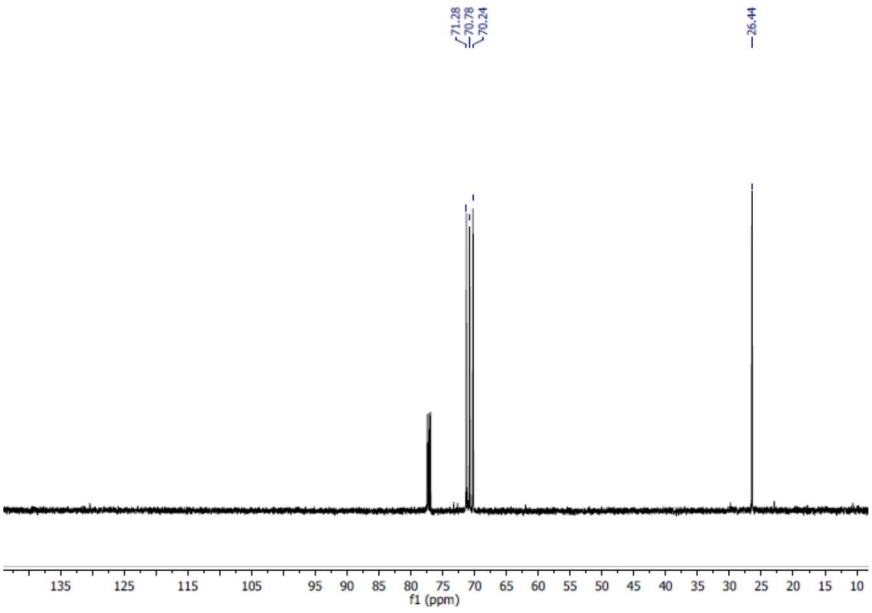

Figure 8. ^{13}C NMR spectrum of $[C_2EO_5]_n$ polymer in $CDCl_3$.

1.5.5 NMR Spectra of Unsaturated $[C_4EO_4\pi]_n$

^{1}H NMR spectrum in ppm ($CDCl_3$, 500 MHz): δ 5.87-5.76 (m, endgroup); 5.53-5.41 (m, 2H); 5.13-4.97 (m, endgroup); 3.69-3.56 (m, 13H); 3.46 (td, J = 7.1, 1.5 Hz, 4H); 2.35 (dd, J = 12.7, 7.1 Hz, 2H); 2.28 (dt, J = 7.1, 6.3 Hz, 2H). ^{13}C NMR spectrum in ppm ($CDCl_3$, 125 MHz): δ 128.50, 127.64, 71.26, 70.98, 70.75, 70.73, 70.71, 70.28, 70.21, 33.18, 28.12.

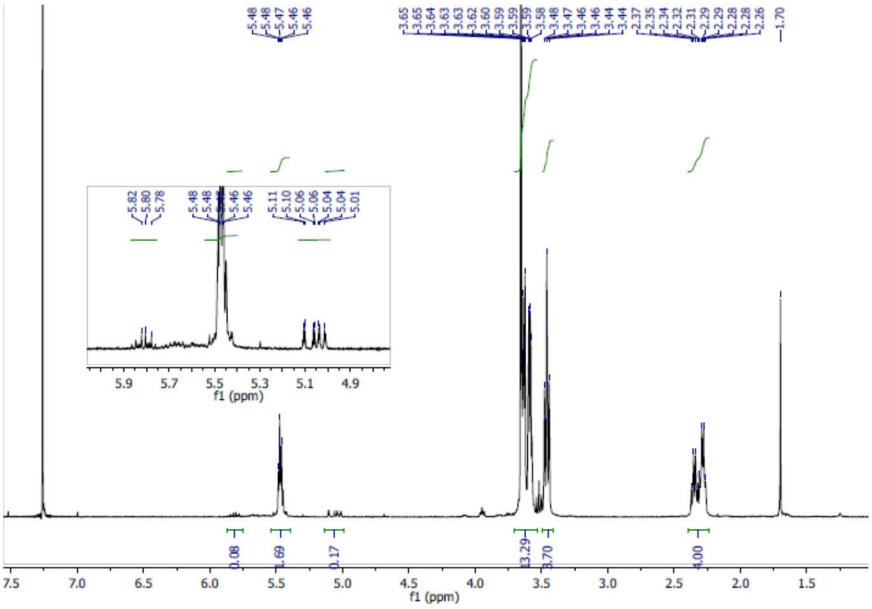

Figure 9. ^{1}H NMR spectrum of unsaturated $[C_4EO_4\pi]_n$ polymer in $CDCl_3$.

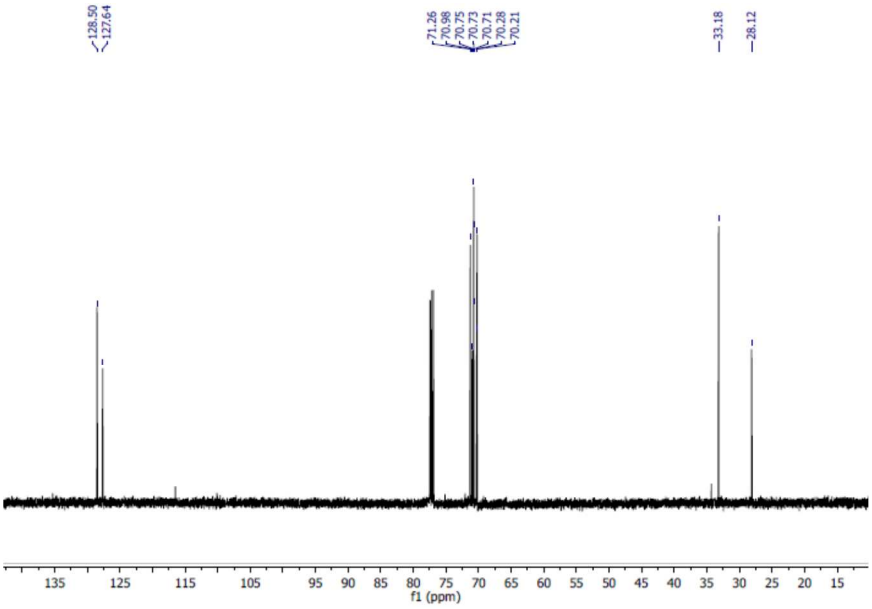

Figure 10. ^{13}C NMR spectrum of unsaturated $[C_4EO_4\pi]_n$ polymer in $CDCl_3$.

1.5.6 NMR Spectra of $[C_4EO_4]_n$

^{1}H NMR spectrum in ppm ($CDCl_3$, 400 MHz): δ 3.68 – 3.53 (m, 12H); 3.43 (t, J = 6.7 Hz, 4H); 1.87 (br s, endgroup); 1.62 – 1.51 (m, 4H); 1.39 – 1.27 (m, 4H); 0.90 (t, J = 7.4 Hz, endgroup). ^{13}C NMR spectrum in ppm ($CDCl_3$, 125 MHz): δ 71.54, 70.73, 70.72, 70.18, 29.72, 26.10.

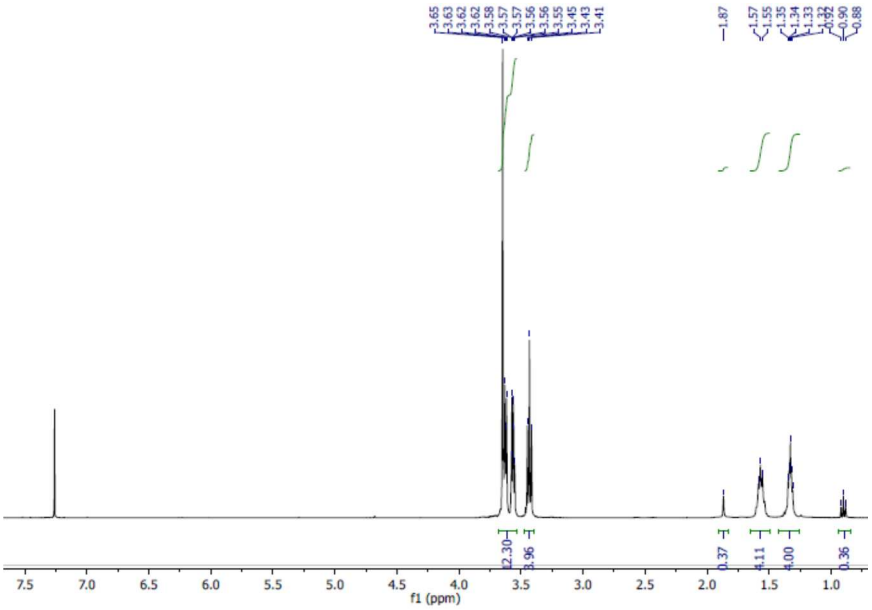

Figure 11. ^{1}H NMR spectrum of $[C_4EO_4]_n$ polymer in $CDCl_3$.

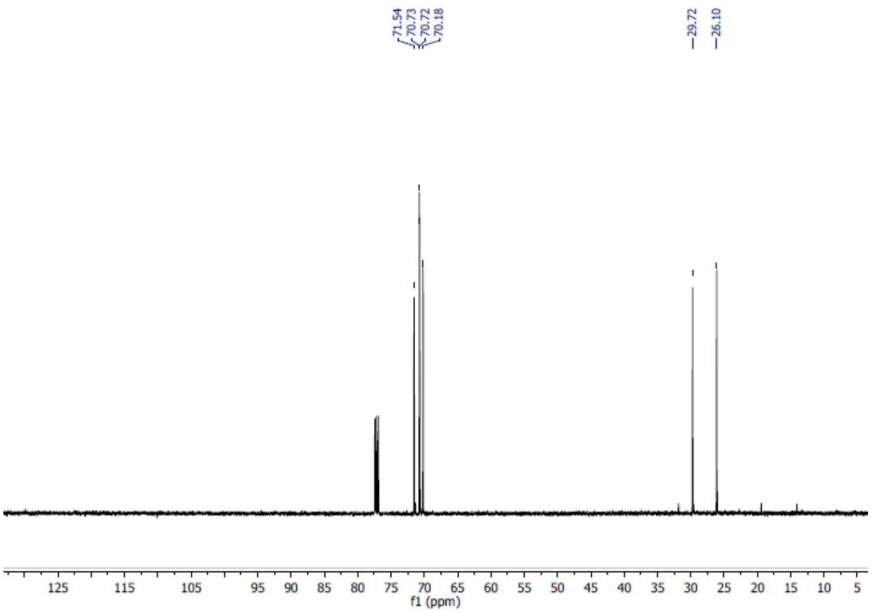

Figure 12. ^{13}C NMR spectrum of $[C_4EO_4]_n$ polymer in $CDCl_3$.

1.5.7 NMR Spectra of Unsaturated $[C_4EO_5\pi]_n$

^{1}H NMR spectrum in ppm ($CDCl_3$, 400 MHz): δ 5.88-5.75 (m, endgroup); 5.53-5.40 (m, 2H); 5.14-4.98 (m, endgroup); 3.66-3.55 (m, 17H); 3.45 (td, J = 7.1, 1.5 Hz, 4H); 2.34 (dd, J = 12.7, 7.0 Hz, 2H); 2.28 (ddd, J = 10.8, 7.0, 1.4 Hz, 1H), 1.70 (dd, J = 6.3, 1.3 Hz, endgroup). ^{13}C NMR spectrum in ppm ($CDCl_3$, 125 MHz): δ 128.48, 127.63, 71.25, 70.97, 70.71, 70.26, 70.20, 33.16, 28.10.

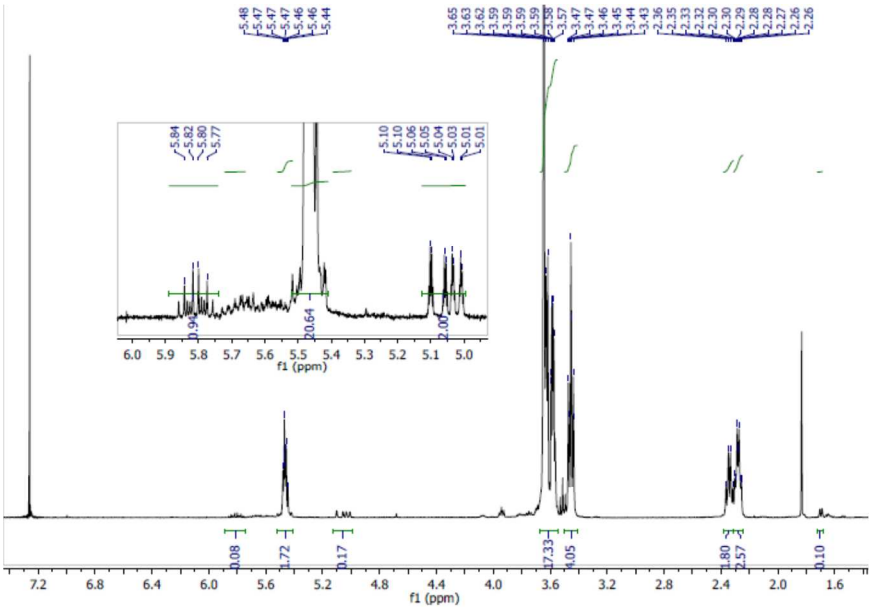

Figure 13. ^{1}H NMR spectrum of unsaturated $[C_4EO_5\pi]_n$ polymer in $CDCl_3$.

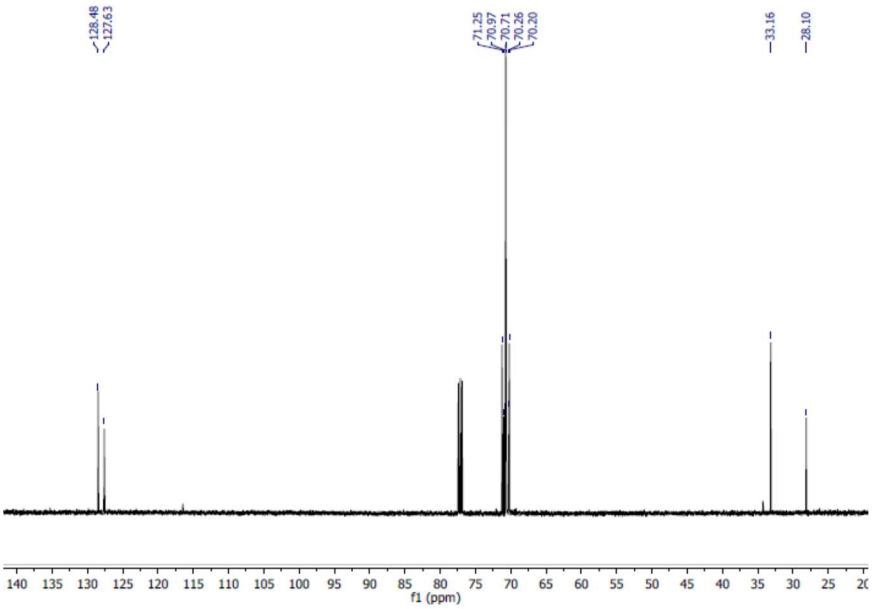

Figure 14. ^{13}C NMR spectrum of unsaturated $[C_4EO_5\pi]_n$ polymer in $CDCl_3$.

1.5.8 NMR Spectra of $[C_4EO_5]_n$

^{1}H NMR spectrum in ppm ($CDCl_3$, 400 MHz): 3.68-3.53 (m, 4H); 3.44 (t, J = 6.8 Hz, 4H); 1.65-1.50 (m, 2H); 1.42-1.25 (m, 2H); 0.91 (t, J = 7.4 Hz, endgroup). ^{13}C NMR spectrum in ppm ($CDCl_3$, 125 MHz): δ 71.57, 70.75, 70.72, 70.19, 29.74, 26.12.

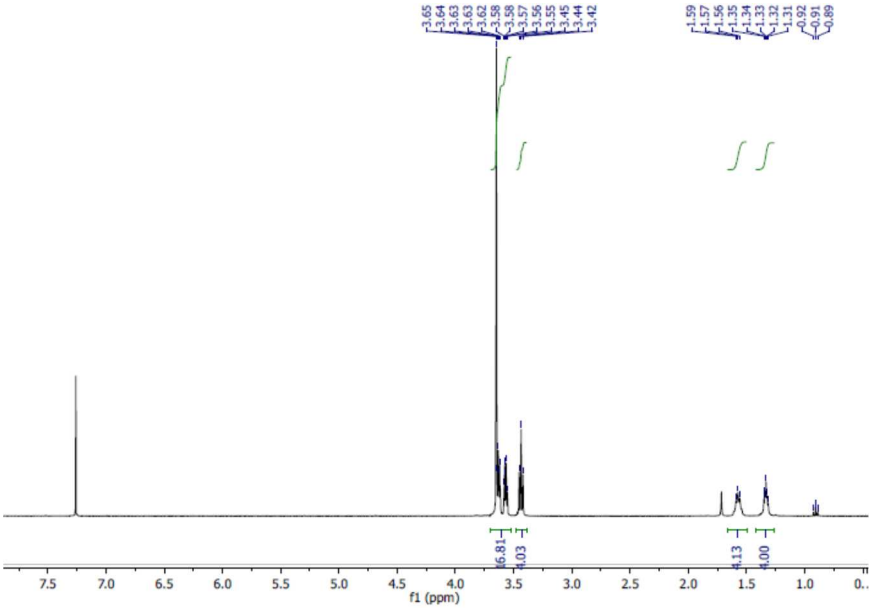

Figure 15. ^{1}H NMR of $[C_4EO_5]_n$ polymer in $CDCl_3$.

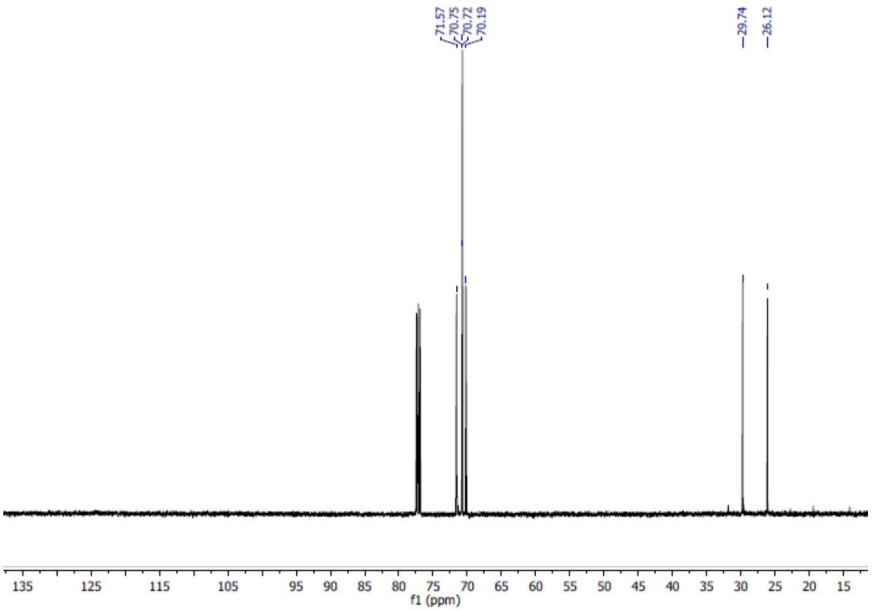

Figure 16. ^{13}C NMR spectrum of $[C_4EO_5]_n$ polymer in $CDCl_3$.

1.5.9 NMR Spectra of Unsaturated $[C_6EO_4\pi]_n$

^{1}H NMR spectrum in ppm ($CDCl_3$, 400 MHz): δ 5.87-5.75 (m, endgroup); 5.46-5.37 (m, *trans* alkene, 2H when combined with *cis*-alkene); 5.36 (t, J = 4.6 Hz, *cis*-alkene); 5.06-4.90 (m, endgroup); 3.69-3.51 (m, 12H); 3.44 (td, J = 6.7, 2.1 Hz, 4H); 2.21-1.92 (m, 4H); 1.70-1.56 (m, 4H). ^{13}C NMR spectrum in ppm ($CDCl_3$, 125 MHz): δ 130.14, 129.72, 70.97, 70.74, 70.24, 70.22, 29.70, 29.58, 29.16, 23.82.

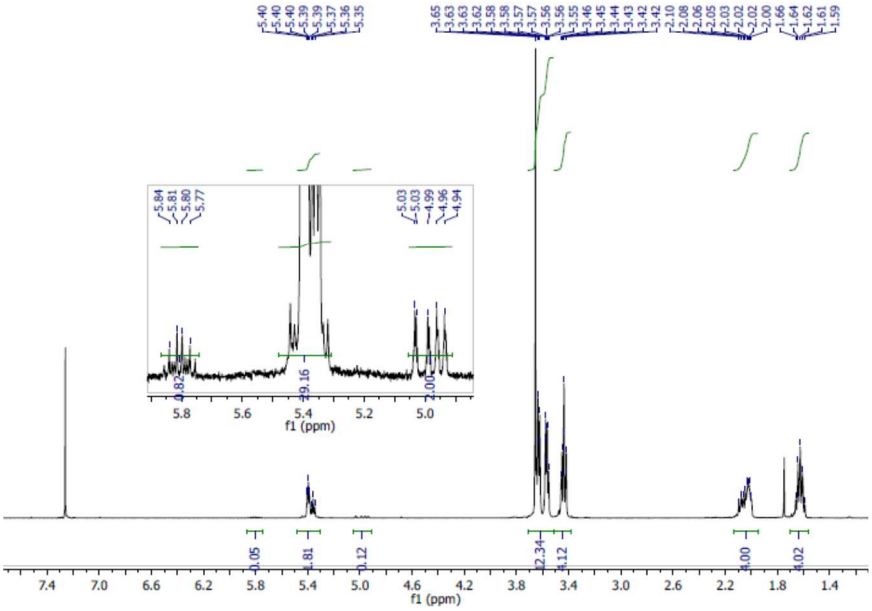

Figure 17. ^{1}H NMR of unsaturated $[C_6EO_4\pi]_n$ polymer in $CDCl_3$.

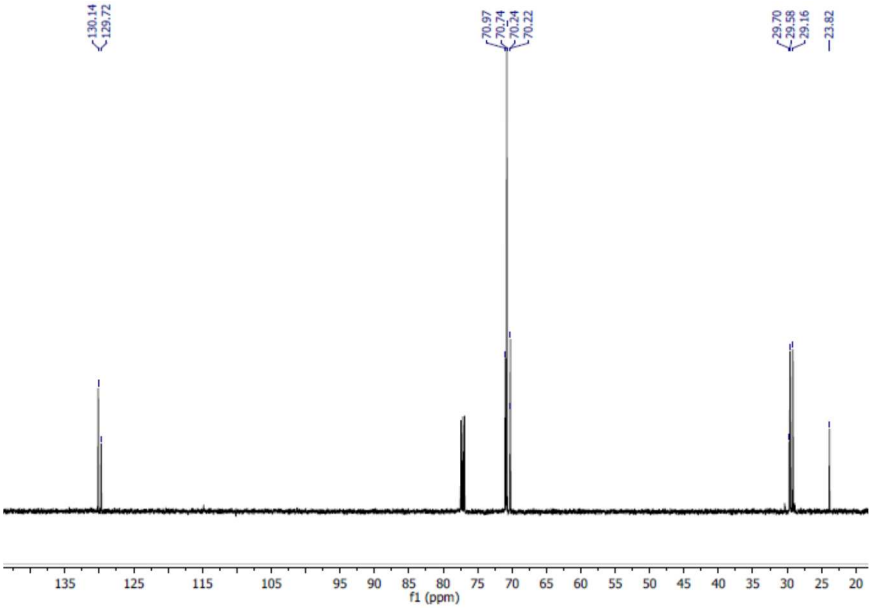

Figure 18. ^{13}C NMR spectrum of unsaturated $[C_6EO_4\pi]_n$ polymer in $CDCl_3$.

1.5.10 NMR Spectra of $[C_6EO_4]_n$

^{13}H NMR spectrum in ppm ($CDCl_3$, 400 MHz): 3.69-3.53 (m, 12H); 3.43 (t, J = 6.8 Hz, 4H); 1.80 (br s, endgroup); 1.62-1.49 (m, 4H); 1.28 (br s, 8H); 0.88 (br s, endgroup). ^{13}C NMR spectrum in ppm ($CDCl_3$, 125 MHz): δ 71.65, 70.75, 70.73, 70.18, 29.76, 29.58, 26.18.

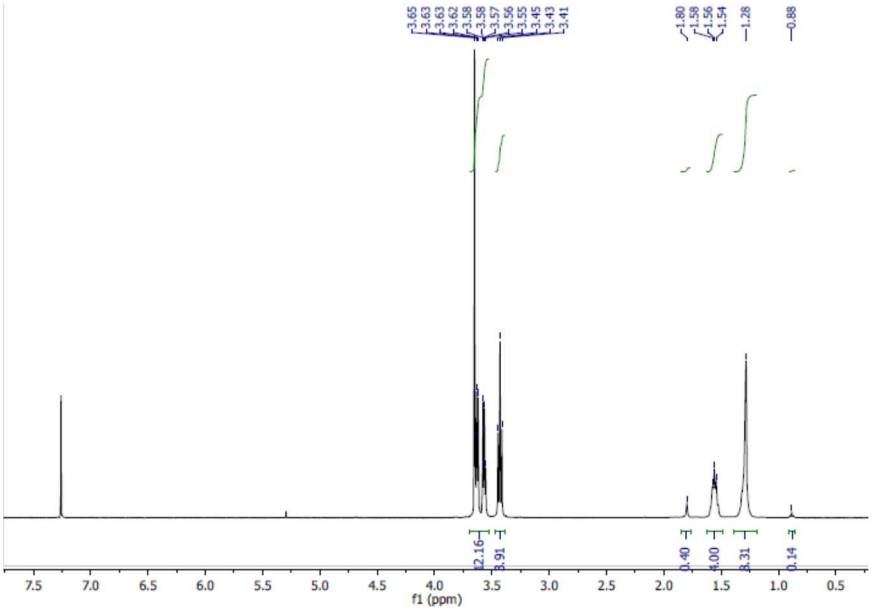

Figure 19. ^{1}H NMR spectrum of $[C_6EO_4]_n$ polymer in $CDCl_3$.

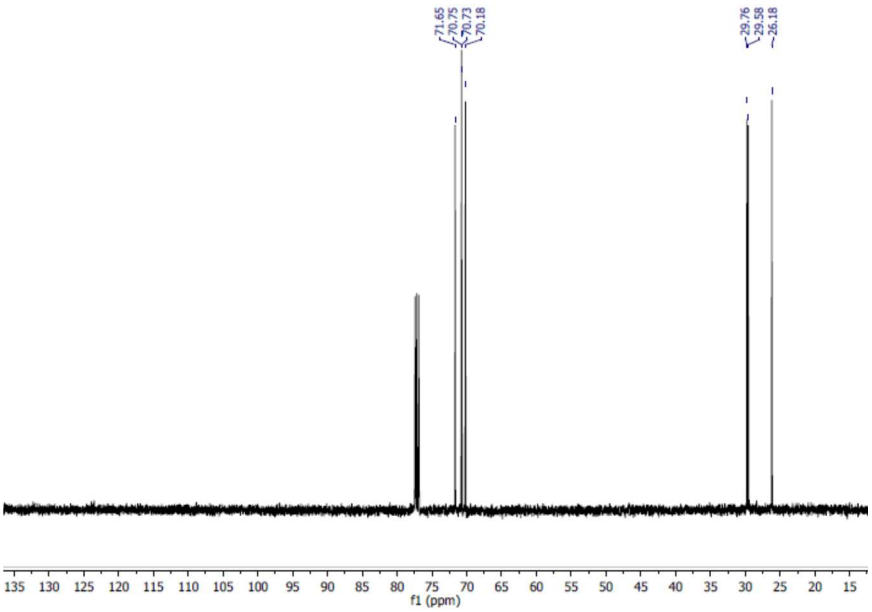

Figure 20. ^{13}C NMR spectrum of $[C_6EO_4]_n$ polymer in $CDCl_3$.

1.5.11 NMR Spectra of Unsaturated $[C_6EO_5\pi]_n$

^{1}H NMR spectrum in ppm ($CDCl_3$, 400 MHz): δ 5.87-5.74 (m, endgroup); 5.43-5.36 (m, *trans* alkene, 2H when combined with *cis*-alkene), 5.36 (t, J = 4.6 Hz, *cis*-alkene); 5.13-4.98 (m, endgroup); 3.67-3.54 (m, 17H); 3.44 (td, J = 6.7, 2.2 Hz, 4H); 2.43-2.22 (m, 4H); 1.68-1.56 (m, 4H). ^{13}C NMR spectrum in ppm ($CDCl_3$, 125 MHz): δ 130.14, 129.72, 70.97, 70.74, 70.24, 70.22, 29.70, 29.58, 29.15, 23.82.

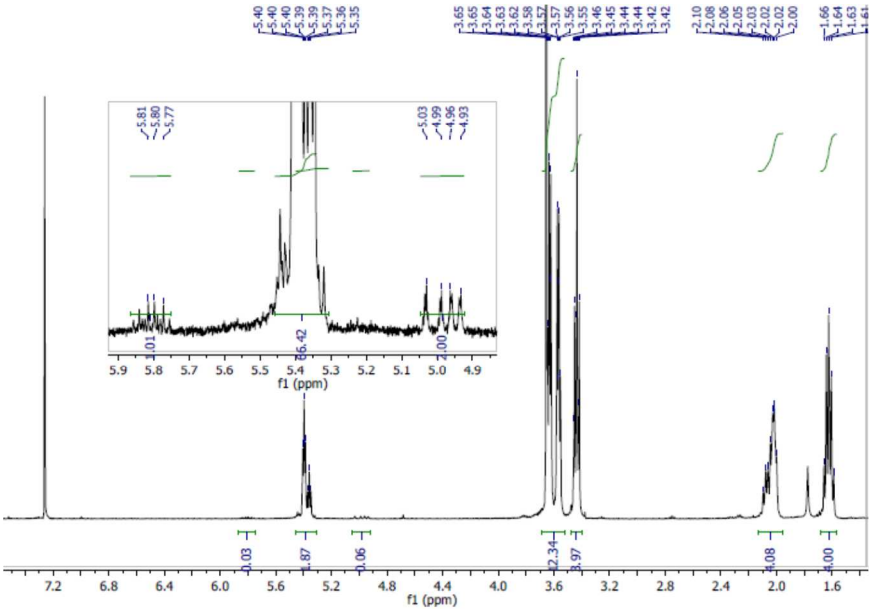

Figure 21. ^{1}H NMR spectrum of $[C_6EO_5\pi]_n$ polymer in $CDCl_3$.

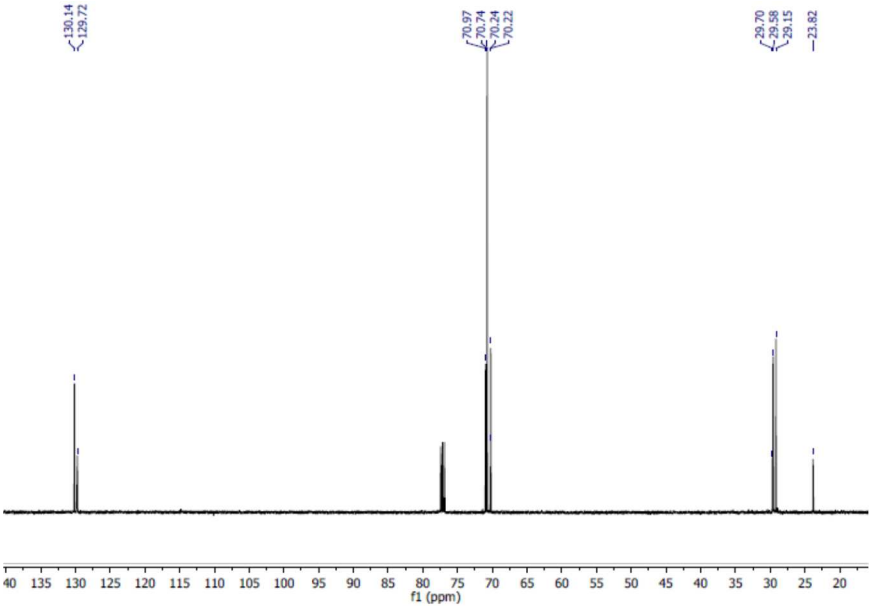

Figure 22. ^{13}C NMR spectrum of $[C_6EO_5\pi]_n$ polymer in $CDCl_3$.

1.5.12 NMR Spectra of $[C_6EO_5]_n$

^{1}H NMR spectrum in ppm ($CDCl_3$, 400 MHz): 3.67-3.53 (m, 16H); 3.43 (t, J = 6.8 Hz, 4H); 1.83 (br s, endgroup); 1.64-1.49 (m, 4H); 1.28 (br s, 8H); 0.91-0.84 (m, endgroup). ^{13}C NMR spectrum in ppm ($CDCl_3$, 125 MHz): δ 71.66, 70.74, 70.71, 70.18, 29.75, 29.58, 26.18.

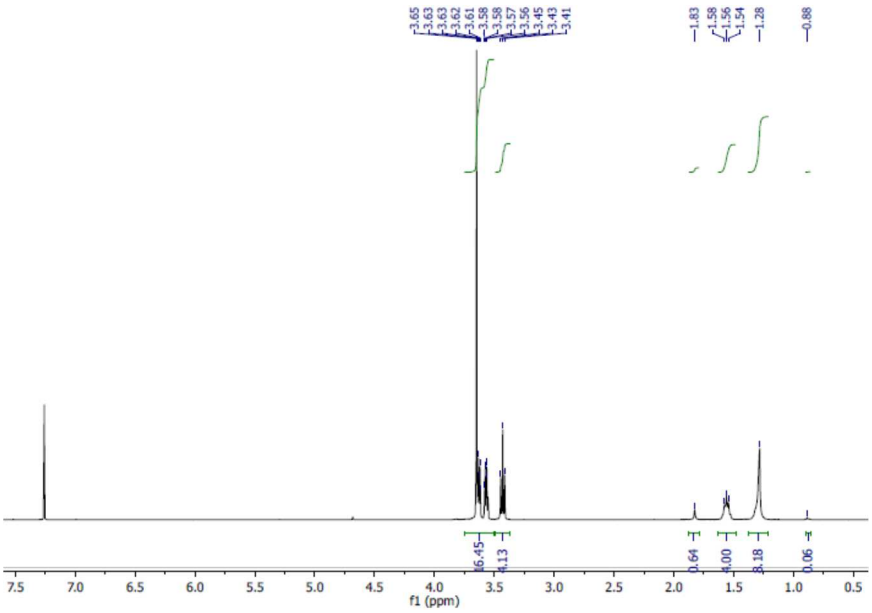

Figure 23. ^{1}H NMR spectrum of $[C_6EO_5]_n$ polymer in $CDCl_3$.

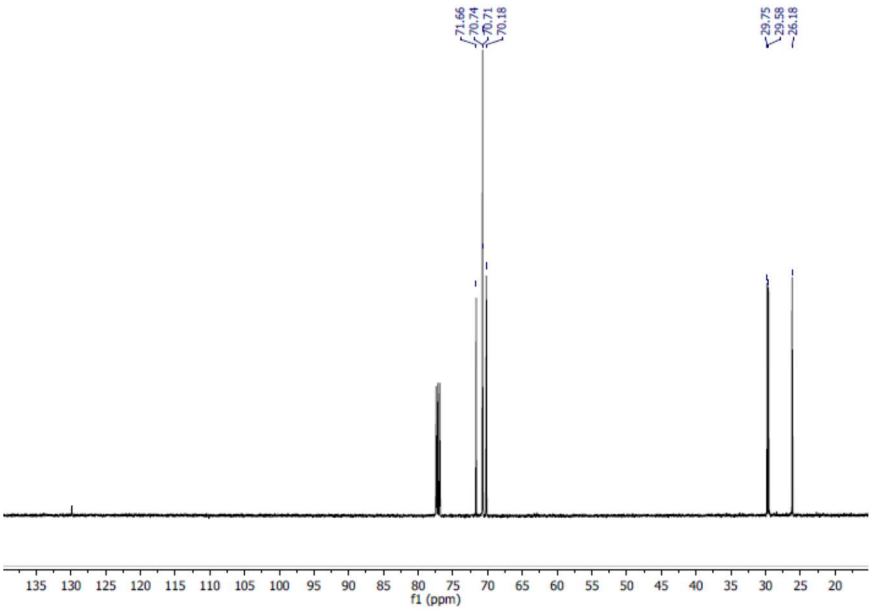

Figure 24. ^{13}C NMR spectrum of $[C_6EO_5]_n$ polymer in $CDCl_3$.

1.6 Analysis of Polymer Endgroups

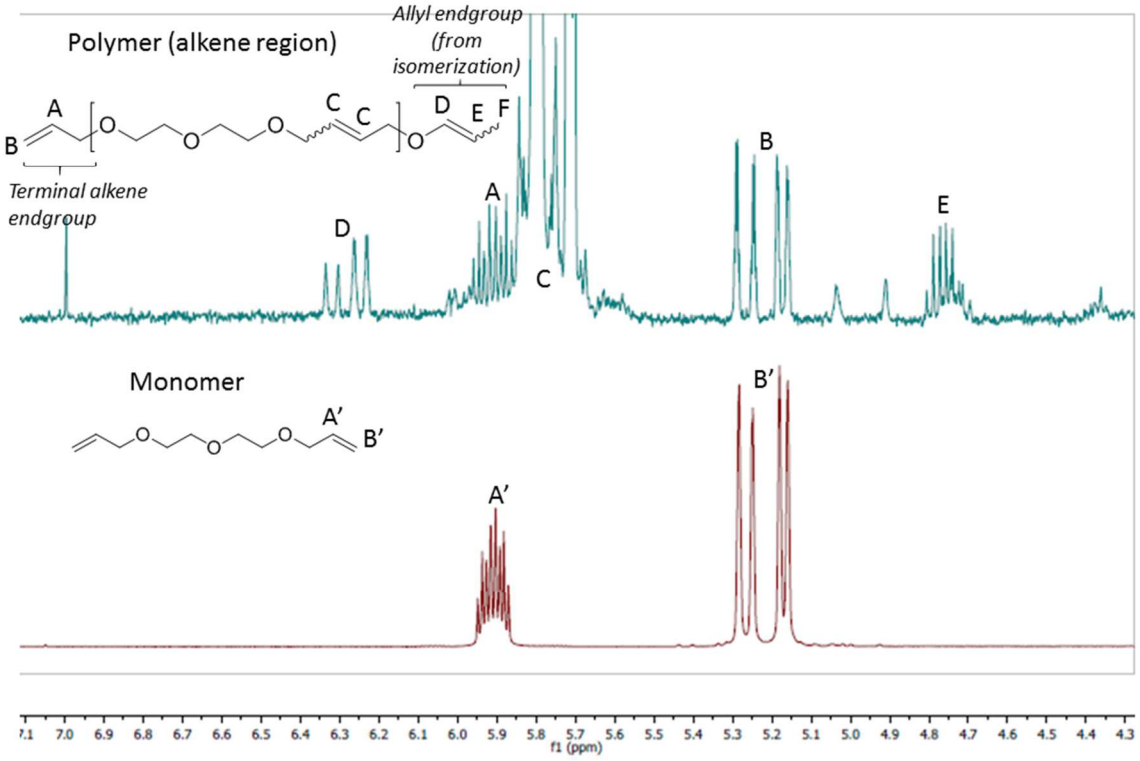

Figure 25. Comparing terminal olefin and allyl ether endgroups in $[C_2EO_3\pi]_n$ polymer.

Grubbs metathesis catalysts are known to form ruthenium hydride species that can lead to side reactions, resulting in the migration of olefins. In the case of the polymers with 1 methylene unit between the ethylene glycol and the alkene, the migration of the olefin would result in the formation of an allyl ether. Depending on the polymerization conditions, we were able to see varying amounts of the allyl ether alkenes in our polymers. Furthermore, when the migration involved the formation of an allyl ether endgroup (vs. an internal allyl ether), we were able to identify a peak (F) at δ 1.54 corresponding to the methyl group of the endgroup (see Figure 33). Thus, we were able to quantify the amount of migration of the internal olefin by comparing the integrations of the allyl alkenes (D, E) to the integration of F. For samples with isomerization primarily of endgroups and no internal olefin migration, one would expect to see D/E/F in a 1:1:3 ratios. For samples with significant migration of the internal olefin, the relative ratio of D and E would be much larger. In general, we were able to

eliminate the migration of the internal olefin by avoiding excessive heat and reaction times, as well as using carefully purified monomer.

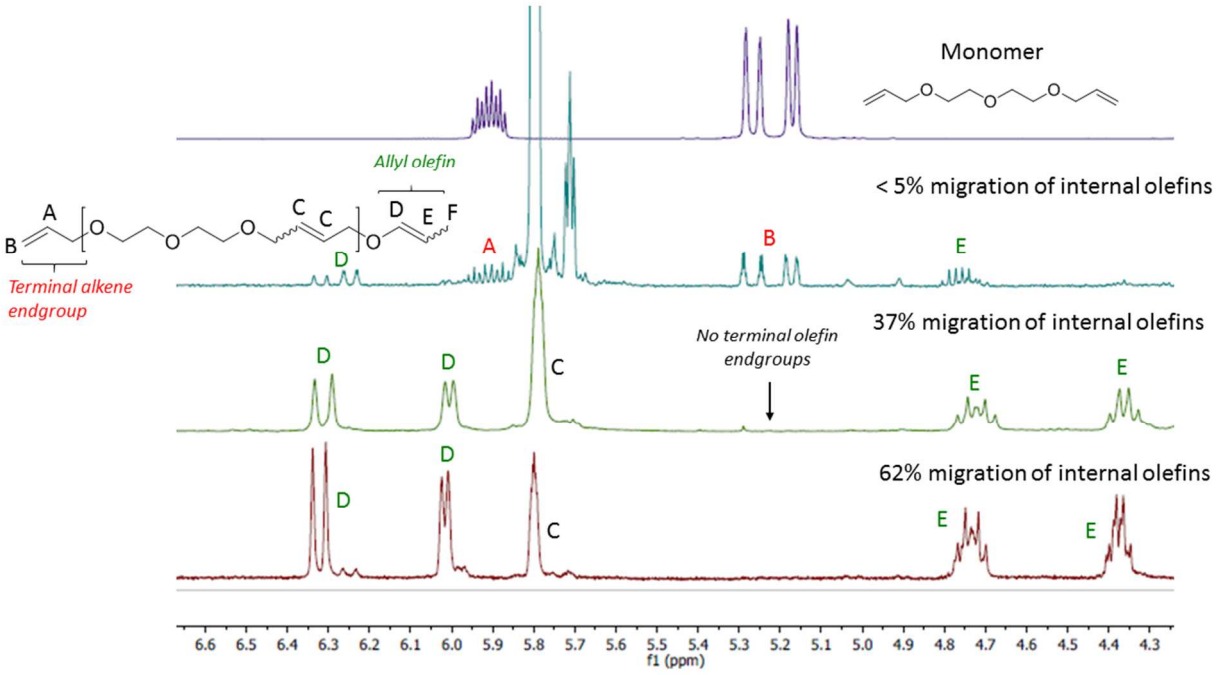

Figure 26. Observation of internal olefin migration by ^{1}H NMR in $[C_2EO_3\pi]_n$ polymer.

1.7 Analysis of Polymer Thermal Stability

1.7.1 Representative TGA Thermograms

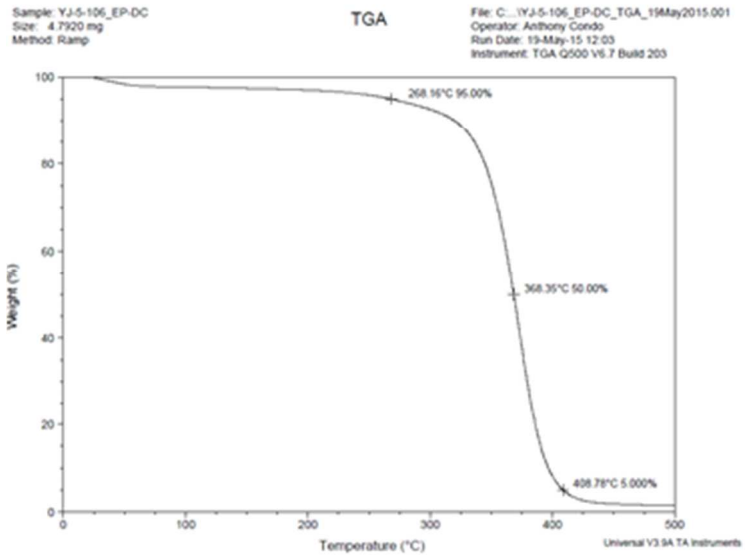

Figure 27. TGA thermogram of unsaturated $[C_2EO_4\pi]_n$ polymer.

Weight% Remaining	95	50	5
Temperature (°C)	286.16	368.35	408.78

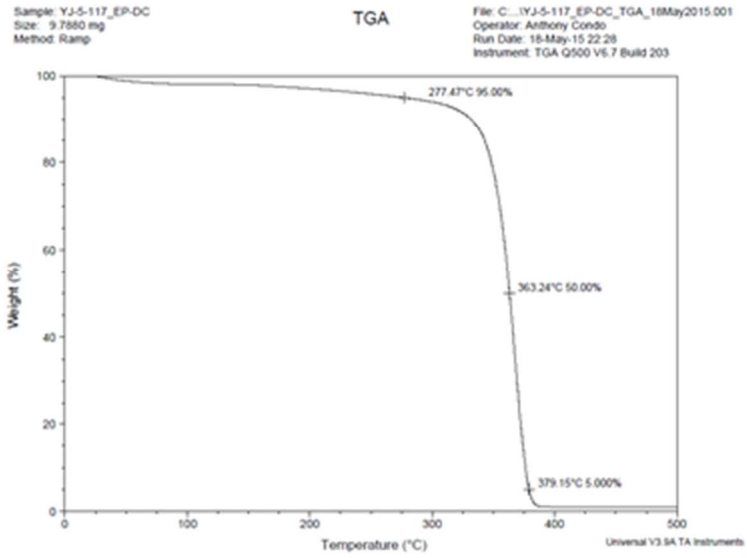

Figure 28. TGA thermogram of $[C_2EO_4]_n$ polymer.

Weight% Remaining	95	50	5
Temperature (°C)	277.47	363.24	379.15

2 Force Field Parameters for Molecular Dynamics Simulations

In this section, the parameters used to perform the MD simulations are provided. As discussed in the main text, the generalized CHARMM bonding parameters are used,[6] and the TraPPE-UA force field[7] is used for all other inter- and intramolecular interactions between polymer atoms. Parameters for the lithium cation are obtained from a previous simulation study.[8] Figure 29 provides reference labels for the different atom types for assigning the appropriate force field parameters.

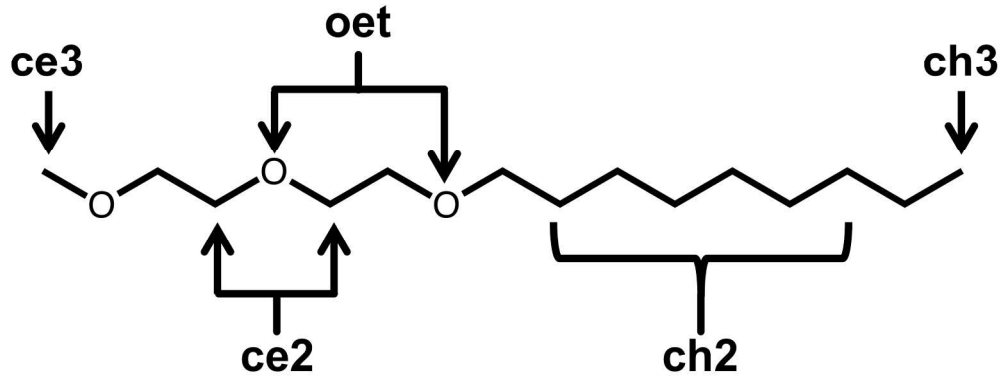

Figure 29. Labels for atom types referenced for force field parameters.

2.1 Non-bonded Interaction Parameters

Non-bonded interactions are computed for all intermolecular interactions and for intramolecular interactions between atoms separated by four or more bonds and consist of pairwise additive Lennard-Jones and Coulombic potentials,

$$u_{\mathrm{nb}}(r_{ij}) = 4\epsilon_{ij}\left[\left(\frac{\sigma_{ij}}{r_{ij}}\right)^{12} - \left(\frac{\sigma_{ij}}{r_{ij}}\right)^{6}\right] + \frac{q_i q_j}{4\pi\varepsilon_0 r_{ij}}, \quad (1)$$

where i and j denote non-bonded atoms, q_i and q_j are their respective partial charges, r_{ij} is the separation distance, σ_{ij} is the Lennard-Jones diameter, and ϵ_{ij} is the Lennard-Jones well depth. Unlike interactions are computed with Lorentz-Berthelot mixing rules:

$$\sigma_{ij} = 0.5\left(\sigma_{ii} + \sigma_{jj}\right) \text{ and } \sigma_{ij} = \sqrt{\epsilon_i \epsilon_j}. \quad (2)$$

Coulombic interactions between atoms separated by three bonds (1-4 interactions) are additionally computed, but the strength of the interaction is reduced by a factor of 0.5, unless otherwise noted. The parameters used in the MD simulations for these interactions are provided in Table 1.

Table 1. Non-bonded potential parameters

atom	m (amu)	σ_{ii} (Å)	ϵ_{ii} (kcal/mol)	q (e)
ch2	14.02694	3.950	0.091411	0.00
ch3	15.03491	3.750	0.194746	0.00
ce2	14.02694	3.950	0.091411	0.25
ce3	15.03491	3.750	0.194746	0.25
oet	15.99940	2.800	0.109296	-0.50
Li^+	6.94100	1.400	0.400000	1.00

2.2 Bonding Potential Parameters

United atoms separated by a single bond interact via a harmonic bonding potential,

$$u_{\text{bond}}(r_{ij}) = k_{\text{bond}}\left(r_{ij} - r_{ij}^{(0)}\right)^2, \quad (3)$$

where k_{bond} is the bonding force constant, r_{ij} is the separation distance between atom i and j, and $r_{ij}^{(0)}$ is the corresponding equilibrium bonding distance. The parameters used in the MD simulations for this type of interaction are provided in Table 2.

Table 2. Bonding potential parameters for polymer atoms.

bond	$k_{\text{bend}}\left(\frac{\text{kcal}}{\text{mol}\cdot\text{Å}^2}\right)$	$r_{ij}^{(0)}$ (degrees)
ce2-ce2	225.0	1.540
ce2-ch2	225.0	1.540
ce2-ch3	225.0	1.540
ce2-oet	360.0	1.410
ce3-oet	360.0	1.410
ch2-ch2	225.0	1.540

2.3 Bending Potential Parameters

United atoms separated by a two bonds interact via a harmonic bending potential,

$$u_{\text{bend}}(\theta_{ijk}) = k_{\text{bend}}\left(\theta_{ijk} - \theta_{ijk}^{(0)}\right)^2, \tag{4}$$

where k_{bend} is the bending force constant, θ_{ijk} is the angle between atom i, j, and k, and $\theta_{ijk}^{(0)}$ is the corresponding equilibrium angle. The parameters used in the MD simulations for this type of interaction are provided in Table 3.

Tables 3. Bending potential parameters for polymer atoms.

bend	$k_{\text{bend}}\left(\frac{\text{kcal}}{\text{mol}\cdot\text{rad}^2}\right)$	$\theta_{ijk}^{(0)}$ (degrees)
ce2-ce2-oet	49.9782	112.0
ce2-ch2-ch2	62.1001	114.0
ce2-oet-ce2	60.0136	112.0
ce3-oet-ce2	60.0136	112.0
ch2-ce2-oet	49.9782	112.0
ch2-ch2-ch2	62.1001	114.0
ch2-ch2-ch3	62.1001	114.0

2.3 Torsional Potential Parameters

United atoms separated by three bonds interact via potential given by a cosine series,

$$u_{\text{tors}}(\phi_{ijkl}) = c_1[1 + \cos(\phi_{ijkl})] + c_2[1 - \cos(2\phi_{ijkl})] + c_3[1 + \cos(3\phi_{ijkl})], \tag{5}$$

where c_1, c_2, and c_3 are constant coefficients, ϕ_{ijkl} is the dihedral angle defined by atoms i, j, k, and l. The parameters used in the MD simulations for this type of interaction are provided in Table 4.

Table 4. Torsional potential parameters for polymer atoms.

torsion	c_1 **(kcal/mol)**	c_2 **(kcal/mol)**	c_3 **(kcal/mol)**
ce2-ce2-oet-ce2	1.44142	-0.32540	1.10926
ce2-ce2-oet-ce3	1.44142	-0.32540	1.10926
ce2-ch2-ch2-ch2	0.70551	-0.13551	1.57251
ce2-oet-ce2-ch2	1.44142	-0.32540	1.10926
ch2-ch2-ch2-ch3	0.70551	-0.13551	1.57251
ch2-ch2-ce2-oet	0.35098	-0.10600	1.53001
ch3-ch2-ce2-oet	0.35098	-0.10600	1.53001
oet-ce2-ce2-oet	0.00000	-0.50002	2.00006

3 Derivation of f_{exp} Formula

As indicated in the *Results and Discussion* section of the main text, the experimental solvation-site connectivity, f_{exp}, quantifies differences in conductivity that arise due to differences in monomer structure, as opposed to those due to shifts in the glass transition temperature T_g or the number of charge carriers. To show this, we take f_{exp} to be the ratio of reduced molar conductivities:

$$f_{\mathrm{exp}} = \left(\frac{\tilde{\sigma}_{\mathrm{r}}}{\tilde{\sigma}_{\mathrm{r,PEO}}}\right)_{r,T-T_{\mathrm{g}}}, \tag{6}$$

where $\tilde{\sigma}_{\mathrm{r}} = \sigma_{\mathrm{r}}/c_{\mathrm{salt}}$, σ_{r} is the reduced conductivity as defined in the main text, c_{salt} is the molar concentration of salt, and $(\ldots)_{r,T\text{-}T_g}$ denotes quantities obtained for a given r = [Li$^+$]/[O] and T-T_g. In eq. 6, utilizing the reduced conductivities enables comparison between polymers at the same T-T_g, and normalizing the conductivity by the concentration reports the mobility of ions in the system rather than the net conductivity. Eq. 6 can then be rewritten in terms of the reduced conductivity and a ratio of the salt concentration in the two electrolytes:

$$f_{\mathrm{exp}} = \left(\frac{\sigma_{\mathrm{r}}}{\sigma_{\mathrm{r,PEO}}}\right)_{r,T-T_{\mathrm{g}}}\left(\frac{c_{\mathrm{salt,PEO}}}{c_{\mathrm{salt}}}\right) = \left(\frac{\sigma_{\mathrm{r}}}{\sigma_{\mathrm{r,PEO}}}\right)_{r,T-T_{\mathrm{g}}}\left(\frac{n_{\mathrm{salt,PEO}}/V}{n_{\mathrm{salt}}/V}\right), \tag{7}$$

where n_{salt} indicates the moles of salt added to the system with total volume V.

For the C$_x$EO$_y$ polymers, it is useful to express n_{salt} in terms of r,

$$n_{\mathrm{salt}} = y n_{\mathrm{mon}} r, \tag{8}$$

and V in terms of the partial molar volumes of the system components,

$$V = n_{\mathrm{mon}}\left[(x+2y)\bar{v}_{\mathrm{CH_2}} + y\bar{v}_{\mathrm{O}}\right] + \textstyle\sum_k n_{\mathrm{salt}}^{(k)}\bar{v}_{\mathrm{salt}}^{(k)}, \tag{9}$$

where $\bar{v}_{\mathrm{CH_2}}$ and $\bar{v}_{\mathrm{O}}$ are the partial molar volumes for a methylene group and an oxygen, respectively, and the summation accounts for the volume of all salt species (free ions, pairs, and aggregates). If the contribution of the salt to the volume is neglected as an approximation, then eq. 7 can be rewritten as

$$f_{\mathrm{exp}} = \left(\frac{\sigma_{\mathrm{r}}}{\sigma_{\mathrm{r,PEO}}}\right)_{r,T-T_{\mathrm{g}}}\left(\frac{\left[(x+2y)\bar{v}_{\mathrm{CH_2}} + y\bar{v}_{\mathrm{O}}\right]}{y\left[2\bar{v}_{\mathrm{CH_2}} + \bar{v}_{\mathrm{O}}\right]_{\mathrm{PEO}}}\right), \tag{10}$$

where the subscript 'PEO' denotes that the partial molar volumes are defined for PEO, in particular. To obtain eq. 4 of the main text, we further approximate that the partial molar volumes of all heavy-atom, backbone moeities are the same with respect to each other (i.e., $\bar{v} = \bar{v}_{\mathrm{CH_2}} = \bar{v}_{\mathrm{o}}$) and also that the partial molar volumes are the same for all C_xEO_y polymers and PEO such that eq. 10 becomes

$$f_{\mathrm{exp}} = \left(\frac{\sigma_{\mathrm{r}}}{\sigma_{\mathrm{r,PEO}}}\right)_{r,T-T_{\mathrm{g}}} \left(\frac{x_{\mathrm{o,PEO}}}{x_{\mathrm{o}}}\right). \tag{11}$$

We note that eq. 10 can also be written with a slightly less stringent approximation ($\bar{v}_{\mathrm{O}}$ in the the C_xEO_y polymers is the same as in PEO) as

$$f_{\mathrm{exp}} = \left(\frac{\sigma_{\mathrm{r}}}{\sigma_{\mathrm{r,PEO}}}\right)_{r,T-T_{\mathrm{g}}} \left(\frac{\phi_{\mathrm{o,PEO}}}{\phi_{\mathrm{o}}}\right), \tag{12}$$

where ϕ_{o} is the volume fraction of oxygen in the polymer electrolyte.

4 Electrolyte Characterization at Different Salt Concentrations

Figure 30 shows conductivity, T_g and reduced conductivity for all electrolytes prepared in this experiment. In Figure 30c, we find that factoring out the effect of T_g on σ organizes the data at all r, consistent with Figure 4 in the main text.

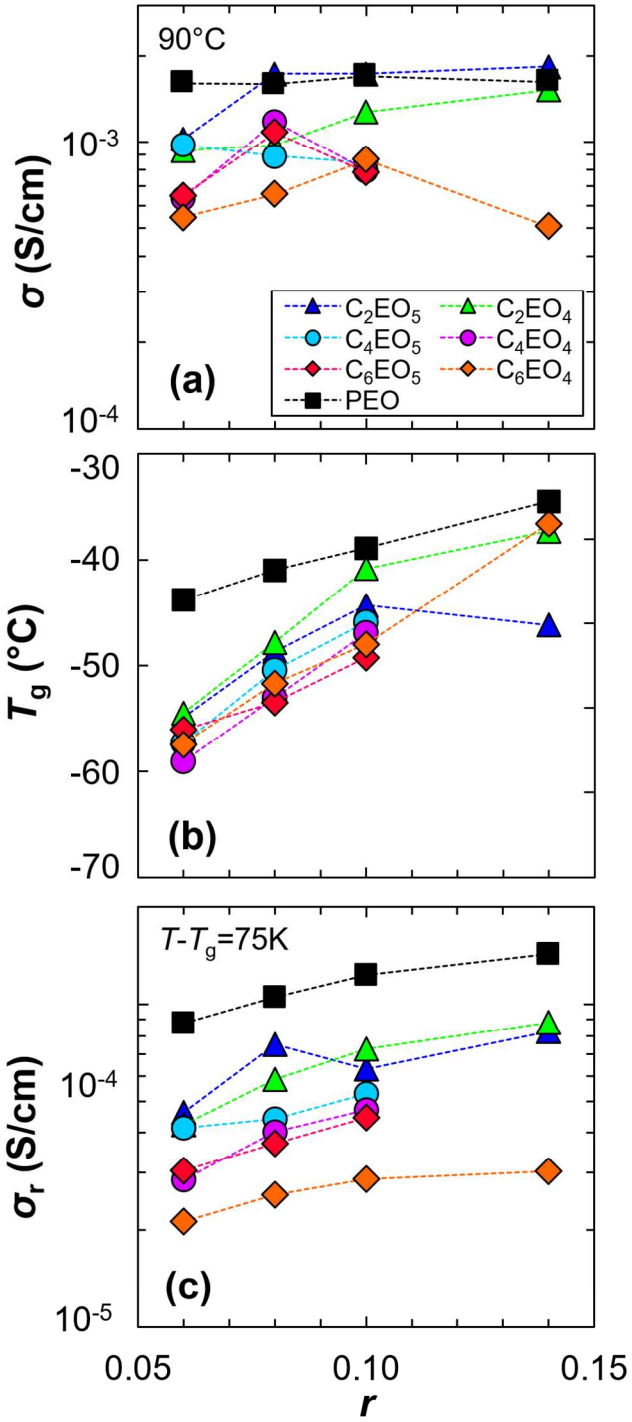

Figure 30. (a) Conductivity, σ, at 90 °C and (b) glass transition temperature, T_g, and (c) reduced conductivity, σ_r, with increasing r.

5 Approximating Conductivity Using the Universal Equation

As described in the *Conclusions* section of the main text, the relationship between f_{exp} and x_o leads us to a universal equation,

$$\sigma\left(r, T - T_{g,PEO} + T_g\right) = \sigma_{PEO}(r, T) \times (3x_o) \times (5.39x_o - 0.86), \quad (13)$$

that can be used to approximate ionic conductivity of any polyether mixed with LiTFSI salt. This approximation relies on four parameters: x_o, the mol fraction of the polymer of interest, $\sigma_{PEO}(r,T)$, the conductivity of PEO at a known temperature and salt concentration, $T_{g,PEO}$, the T_g of PEO at r; and T_g, the T_g of the electrolyte of interest at r. The conductivity approximated using eq. 13 will be at the same r as σ_{PEO} and at a temperature of T-T_g,PEO+T_g, where T is the temperature of σ_{PEO}. Data for σ_{PEO} and $T_{g,PEO}$ as a function of temperature and salt concentration is well reported in the literature. For convenience, we provide our measurements for σ_{PEO} and $T_{g,PEO}$ at varying r and T. We also provide a method for approximating the T_g of any polyether electrolyte based off of x_o and r, in the case that the T_g of the polymer/salt mixture has not been measured.

The relationship between f_{exp} and theoretical connectivity will depend chain architecture of the polymer, especially in cases where all oxygens are not chemically similar and equally accessible. Thus, further work is required to extend our work to cover electrolytes based on comb or branched polymers. Another instance where we can conceive deviation from this relationship is in an ion-paired system, or one where steric hindrance precludes the solvation of the lithium ion. Also, we do not expect the approximation to capture limitations of ion transport due to the presence of a crystalline phase, as our entire analysis was performed on fully amorphous materials. In these cases, eq. 13 would not provide a good estimate of the electrolyte conductivity.

5.1 Tabulated Data for σ and T_g of PEO

Table 5. Conductivity data for PEO at different temperatures and salt concentrations where r=[Li^+/O]. The last row shows the measured T_g of electrolytes at different salt concentrations. All data was obtained using 5 kg/mol PEO mixed with LiTFSI salt.

T (°C)	r=0.02	r=0.04	r=0.08	r=0.10	r=0.12	r=0.14	r=0.16
27	4.12×10^{-7}	8.14×10^{-7}	7.08×10^{-5}	5.08×10^{-5}	5.37×10^{-5}	3.12×10^{-5}	3.15×10^{-5}
40	2.40×10^{-6}	5.19×10^{-6}	1.67×10^{-4}	1.54×10^{-4}	1.53×10^{-4}	1.03×10^{-4}	9.86×10^{-5}
50	9.49×10^{-6}	3.13×10^{-5}	3.34×10^{-4}	3.11×10^{-4}	2.98×10^{-4}	2.19×10^{-4}	2.04×10^{-4}
60	1.57×10^{-4}	5.00×10^{-4}	5.55×10^{-4}	5.54×10^{-4}	5.33×10^{-4}	4.06×10^{-4}	3.77×10^{-4}
70	4.96×10^{-4}	7.05×10^{-4}	8.00×10^{-4}	8.89×10^{-4}	8.84×10^{-4}	6.92×10^{-4}	7.68×10^{-4}
80	6.27×10^{-4}	9.45×10^{-4}	1.17×10^{-3}	1.31×10^{-3}	1.24×10^{-3}	1.09×10^{-3}	9.80×10^{-4}
90	8.16×10^{-4}	1.22×10^{-3}	1.60×10^{-3}	1.84×10^{-3}	1.76×10^{-3}	1.59×10^{-3}	1.45×10^{-3}
100	9.78×10^{-4}	1.53×10^{-3}	2.10×10^{-3}	2.47×10^{-3}	2.40×10^{-3}	2.23×10^{-3}	2.03×10^{-3}
110	1.18×10^{-3}	1.88×10^{-3}	2.69×10^{-3}	3.18×10^{-3}	-	2.95×10^{-3}	-
T_g (°C)	-55.9	-51.9	-43.7	-38.5	-35.6	-30.9	-27.5

5.2 Approximating the T_g of a Polyether Electrolyte

Figure 31 shows data for the increase in the glass transition temperature, ΔT_g, relative to the neat polymer at varying r. We find that the data falls on a line,

$$\Delta T_g = 222.6\, r, \tag{14}$$

where $\Delta T_g = T_{g,r} - T_{g,neat}$. On average eq. 14 estimates the ΔT_g within 20% for C_xEO_y polymers and will likely provide a good approximation for the T_g at a given value of r for other polyethers, if the T_g of the neat polymer is known.

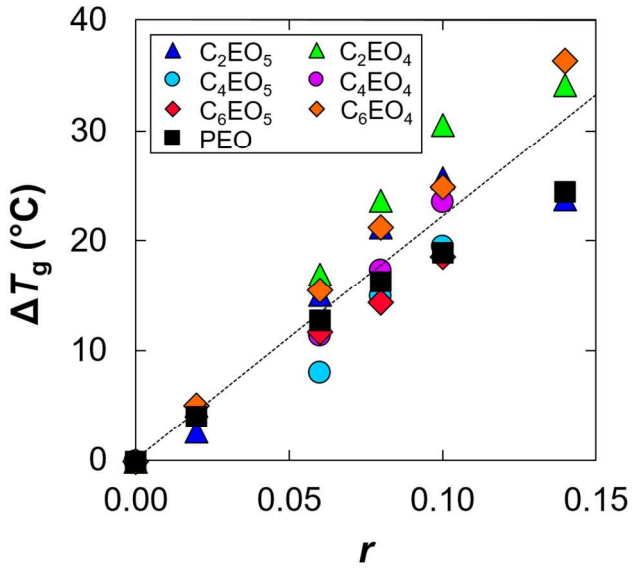

Figure 31. Increase in T_g as a function of salt concentration. The T_g at r=0 is that of the neat polymer.

6 References

(1) Maynard, H. D.; Grubbs, R. H. Synthesis of Functionalized Polyethers by Ring-Opening Metathesis Polymerization of Unsaturated Crown Ethers. *Macromolecules* **1999**, *32* (21), 6917–6924.

(2) Zona, C.; D'Orazio, G.; La Ferla, B. Controlled-Length Efficient Synthesis of Heterobifunctionalized Oligo Ethylene Glycols. *Synlett* **2013**, *24* (06), 709–712.

(3) McFarland, J. M.; Francis, M. B. Reductive Alkylation of Proteins Using Iridium Catalyzed Transfer Hydrogenation. *J. Am. Chem. Soc.* **2005**, *127* (39), 13490–13491.

(4) Kilbinger, A. F. M.; Cantrill, S. J.; Waltman, A. W.; Day, M. W.; Grubbs, R. H. Magic Ring Rotaxanes by Olefin Metathesis. *Angew. Chemie Int. Ed.* **2003**, *42* (28), 3281–3285.

(5) Cho, J. H.; Kim, B. M. An Efficient Method for Removal of Ruthenium Byproducts from Olefin Metathesis Reactions. *Org. Lett.* **2003**, *5* (4), 531–533.

(6) Vanommeslaeghe, K.; Hatcher, E.; Acharya, C.; Kundu, S.; Zhong, S.; Shim, J.; Darian, E.; Guvench, O.; Lopes, P.; Vorobyov, I.; et al. CHARMM General Force Field: A Force Field for Drug-Like Molecules Compatible with the CHARMM All-Atom Additive Biological Force Fields. *J. Comput. Chem.* **2010**, *31* (4), 671–690.

(7) Stubbs, J. M.; Potoff, J. J.; Siepmann, J. I. Transferable potentials for phase equilibria. 6. United-atom description for ethers, glycols, ketones, and aldehydes. *J. Phys. Chem. B* **2004**, *108* (45), 17596–17605.

(8) Wu, H.; Wick, C. D. Computational Investigation on the Role of Plasticizers on Ion Conductivity in Poly(ethylene oxide) LiTFSI Electrolytes. *Macromolecules* **2010**, *43* (7), 3502–3510.